Cystathionine β-Synthase (CBS) Domain-containing Pyrophosphatase as a Target for Diadenosine Polyphosphates in Bacteria*

Viktor A. Anashkin[‡§], Anu Salminen[‡], Heidi K. Tuominen[‡], Victor N. Orlov[§], Reijo Lahti[‡1], and Alexander A. Baykov[§2]

From the [‡]Department of Biochemistry, University of Turku, FIN-20014 Turku, Finland and the [§]Belozersky Institute of Physico-Chemical Biology and Department of Chemistry, Lomonosov Moscow State University, Moscow 119899, Russia

***Running title:** *Nucleotide-regulated soluble pyrophosphatases*

To whom correspondence may be addressed: Prof. Reijo Lahti, Dept. of Biochemistry, University of Turku, Vatselankatu 2, FIN-20014 Turku, Finland. Tel.: 358-2353-6845; Fax: 358-2353-6860; E-mail: reijo.lahti@utu.fi.

Keywords: Allosteric regulation, Cooperativity, Bacterial signal transduction, Ligand-binding protein, CBS domain, Pyrophosphatase.

Background: Many soluble pyrophosphatases contain two regulatory nucleotide-binding CBS domains with or without an intercalating DRTGG domain.
Results: Linear P^1,P^n-diadenosine 5′-polyphosphates (Ap_nAs, n = 3–6) bind with nanomolar affinity to and activate DRTGG domain-containing pyrophosphatases; Ap_3A binds cooperatively.
Conclusion: Nucleotide-regulated pyrophosphatases may represent receptors for Ap_nAs in bacteria.
Significance: The results suggest a novel regulatory pathway in some bacteria, involving Ap_nAs as messengers.

ABSTRACT

Among numerous proteins containing pairs of regulatory cystathionine β-synthase (CBS) domains, Family II pyrophosphatases (CBS-PPases) are unique in that they generally contain an additional DRTGG domain between the CBS domains. Adenine nucleotides bind to the CBS domains in CBS-PPases in a positively cooperative manner, resulting in enzyme inhibition (AMP, ADP) or activation (ATP). Here we show that linear P^1,P^n-diadenosine 5′-polyphosphates (Ap_nAs, where *n* is the number of phosphate residues) bind with nanomolar affinity to DRTGG domain-containing CBS-PPases of *Desulfitobacterium hafniense*, *Clostridium novyi* and *Clostridium perfringens*, and increase their activity up to 30-, 5- and 7-fold, respectively. Ap_4A, Ap_5A and Ap_6A bound non-cooperatively and with similarly high affinities to CBS-PPases, whereas Ap_3A bound in a positively cooperative manner and with lower affinity, like mononucleotides. All Ap_nAs abolished kinetic cooperativity (non-Michaelian behavior) of CBS-PPases. The enthalpy change and binding stoichiometry, as determined by isothermal calorimetry, were approximately 10 kcal/mol nucleotide and 1 mol/mol enzyme dimer for Ap_4A and Ap_5A, but 5.5 kcal/mol and 2 mol/mol for Ap_3A, AMP, ADP and ATP, suggesting different binding modes for the two nucleotide groups. In contrast, *Eggerthella lenta* and *Moorella thermoacetica* CBS-PPases, which contain no DRTGG domain, were not affected by Ap_nAs and showed no enthalpy change, indicating the importance of the DTRGG domain for Ap_nA binding. These findings suggest that Ap_nAs can control CBS-PPase activity and hence affect pyrophosphate level and biosynthetic activity in bacteria.

Diadenosine polyphosphates (Ap_nAs) are ubiquitous compounds in which two adenosine moieties are linked through ribose 5′-C by a chain of 3 to 6 phosphate residues. First discovered in 1965 as byproducts of chemical ATP synthesis (1), they have subsequently been identified in organisms belonging to all kingdoms of life. Many enzymatic reactions leading to Ap_nAs are known

(2), of which the reaction catalyzed by aminoacyl-tRNA synthetase, lysyl-tRNA synthetase (LysRS) in particular (3), is the best known. *Escherichia coli* LysRS produces Ap_nAs by a side reaction during lysyl-tRNA synthesis via attack of the terminal phosphate group of ATP and other monoadenosine phosphates on the enzyme-bound aminoacyl adenylate intermediate (4). Since ATP prevails in cells, the product of its reaction with aminoacyl adenylate, Ap_4A, is the most prevalent Ap_nA. LysRS can additionally convert Ap_4A to Ap_3A (5). Ap_nAs are degraded in the cell by specific and nonspecific enzymes, including Ap_4A hydrolase and phosphodiesterase (6, 7), which balance the intracellular concentration of Ap_nAs at a submicromolar level. However, their concentrations in prokaryotes can rise up to 300 μM under stress conditions (8).

Because of its association with stress, AP_4A was originally classified as an intracellular "alarmone" (8–10). An alternative view is that AP_4A formation represents a compensatory mechanism that helps to sustain basic physiology during stress and assist in the return to normal physiology in bacteria (11). In eukaryotes, Ap_nAs may have a second messenger role (12). Regardless of which theory is true, it is clear that Ap_nAs participate, in some as yet poorly understood ways, in a number of cellular phenomena associated with stress, such as DNA replication and repair (13) and cell division (14). In eukaryotes, Ap_nAs are involved in many other processes, including neurotransmission (15), apoptosis (16), and analgesia (17). Of note, Ap_4A is used in hypoxia therapy in humans (18).

Understanding the roles of Ap_nAs requires knowledge of their target proteins. Using a radioactive photocrosslinking Ap_4A analog, Johnstone and Farr (19) detected 12 Ap_4A-binding proteins in *E. coli* extract, some of which were identified as heat-shock proteins based on their electrophoretic mobilities. Guo et al. (20) and Azhar et al. (21) used pull-down assays with immobilized Ap_4A analogs followed by mass-spectral analysis to identify, respectively, 6 and 13 binding proteins in *E. coli*. The three protein sets obtained in these studies partially overlapped. Few Ap_nA protein complexes have been subjected to biophysical and mechanistic studies. Apart from cases where Ap_nAs act as substrates or products of their metabolizing enzymes, the chaperone GroEL binds Ap_4A with a dissociation constant of 10 μM; the complex exhibits increased ATPase and chaperoning activities (11). Human 5′-nucleotidase II is allosterically activated by Ap_nAs (n = 4–6), which bind with dissociation constants of 60–80 μM (22).

Inorganic pyrophosphatases (PPases; EC 3.6.1.1), the major PP_i-metabolizing enzymes in all types of organisms, belong to three non-homologous families (23). Family II PPases, found in bacteria and archaea, are homodimeric Mn^{2+}- or Co^{2+}-metalloenzymes that additionally require Mg^{2+} for catalysis (24). A quarter of the more than 500 putative Family II PPase sequences contain a regulatory insert comprising a pair of cystathionine β-synthase (CBS) domains (Bateman module (25)) within one of the two catalytic domains. Regulatory CBS domains are found in proteins in all kingdoms of life and generally bind adenine nucleotides as regulating molecules (26−28); mutations in CBS domains of human proteins are associated with hereditary diseases (29, 30). Interestingly, only in CBS-PPases (but not all of them), the CBS domains are intercalated by another (DRTGG) domain. CBS-PPases are activated by ATP and inhibited by AMP and ADP (31, 32). Both catalysis and regulation involve marked positive cooperativity, which is Mg^{2+}-dependent (32).

The structure of the isolated dimeric regulatory insert of *Clostridium perfringens* PPase (*cp*PPase) obtained for crystals grown in the presence of 0.25 mM Ap_4A contains an AP_4A molecule bound by two CBS domain pairs at the subunit interface (33), raising the possibility that Ap_4A may be a physiological ligand of CBS-PPases. Preliminary activity measurements (33, 34) suggested that Ap_4A activates *cp*PPase. Here we show that all AP_nAs bind with nanomolar affinities to three DRTGG-domain–containing CBS-PPases and modulate their catalytic activity and cooperative behavior. Our data thus identify a new type of ligand for CBS domains and an important target of Ap_nAs in the protein world.

Experimental Procedures

Enzymes and Reagents—Genes for CBS-PPases from *Desulfitobacterium hafniense* (*dh*PPase), *Clostridium novyi* (*cn*PPase), *C. perfringens* (*cp*PPase), *Eggerthella lenta* (*el*PPase) and *Moorella thermoacetica* (*mt*PPase) were expressed in *E. coli*, and the produced CBS-PPases were purified as described previously

(32−34). Inactive aggregates were separated from soluble active proteins during size-exclusion chromatography. The final products were at least 95% pure as estimated by SDS-PAGE using a Phast system with 8–25% gradient gels (GE Healthcare). Protein concentrations were determined with a Nanodrop spectrophotometer (Thermo Scientific) using $A^{0.1\%}_{280}$ of 0.478 for *dh*PPase, 0.548 for *cn*PPase, 0.426 for *cp*PPase, 0.493 for *el*PPase and 0.48 for *mt*PPase, as calculated from their amino acid compositions with ProtParam. Molar concentrations were calculated based on subunit molecular masses of 60.4, 63.6, 60.8, 52.5 and 48.1 kDa, respectively. All enzyme concentrations are given in terms of the dimer.

P^1,P^n-diadenosine 5′-polyphosphates (Ap_nAs) with n = 3–5 were from Sigma; Ap_6A was from Jena Bioscience. The concentrations of stock nucleotide solutions were calibrated by measuring absorbance in the ultraviolet region (ε_{259} = 31,800 $M^{-1}\cdot cm^{-1}$ for dinucleotides and 15,900 $M^{-1}\cdot cm^{-1}$ for mononucleotides).

Kinetic Assays—The activity assay medium contained 5 mM $MgCl_2$, 140 μM PP_i (yielding 50 μM $MgPP_i$ complex) and 0.1 M Tes-KOH (pH 7.2), except where specified otherwise. In measurements done at higher Mg^{2+} concentrations, buffer concentration was decreased appropriately to maintain constant ionic strength. The reaction was initiated by adding enzyme, and P_i accumulation due to PP_i hydrolysis was continuously recorded for 2–3 min at 25 °C using an automated P_i analyzer (35). Initial velocities of PPi hydrolysis were typically estimated graphically from the slopes of the tangents to the initial portion of hydrolysis time courses recorded with the P_i analyzer.

Isothermal Calorimetry—A VP-iTC calorimeter (MicroCal Ltd., USA) was used. Enzyme and nucleotide solutions were made in 0.1 M MOPS/KOH (pH 7.2) buffer containing 2 mM $MgCl_2$, 0.1 mM $CoCl_2$, and 150 mM KCl. Titrations were performed at 25 °C by successive 10-μl injections of 0.1−10 mM mononucleotide or 33 μM dinucleotide solution into 2 ml of CBS-PPase solution (2.5−5 μM in terms of the dimer); the interval between injections was 5 min. All samples were degassed before the experiment. Binding isotherms were corrected by subtracting the ligand dilution isotherms, determined by titrating nucleotide solutions into the buffer.

Calculations and Data Analysis—The values of the apparent dissociation constants for the magnesium complexes of PP_i used to calculate free metal ion concentrations at pH 7.2 were 112 μM for $MgPP_i$ and 2.84 mM for Mg_2PP_i (36).

Nonlinear least square fittings were performed using the program Scientist (Micromath). The dependence of hydrolysis rate on nucleotide concentration ([N]) was fit to Equation 1,

$$v = \{v_N + (v_0 + v_N)K_{N2}/2[N] + v_0K_{N1}K_{N2}/[N]^2\}/(1 + K_{N2}/[N] + K_{N1}K_{N2}/[N]^2), \quad \text{(Eq. 1)}$$

where v_0 and v_N are activities of free and nucleotide-saturated enzyme, respectively, and K_{N1} and K_{N2} are the apparent dissociation constants describing successive binding of nucleotide to two regulatory sites per enzyme molecule. Cooperative kinetics of substrate ($MgPP_i$) hydrolysis were analyzed with Equation 2,

$$v = k_{cat}[E]_0(1 + 0.5K_{m2}/[S])/(1 + K_{m2}/[S] + K_{m1}K_{m2}/[S]^2), \quad \text{(Eq. 2)}$$

which assumes different Michaelis constants (K_{m1} and K_{m2}) and equal k_{cat} values for the two active sites in the dimer; $[E]_0$ and [S] are total enzyme and substrate concentrations, respectively. The corresponding binding schemes and details of the fitting procedure were described previously (32).

The dependencies of K_{N1}, K_{N2}, K_{m1} and K_{m2} on Mg^{2+} (M) concentration were fit to Equation 3,

$$K_L = (K_L)_0(1 + [M]/K_M)/\{1 + (K_L)_0[M]/(K_L)_M/K_M\}, \quad \text{(Eq. 3)}$$

where $(K_L)_0$ and $(K_L)_M$ are the limiting values of the respective K_N or K_m at zero and infinite Mg^{2+} concentrations, and K_M is the metal binding constant.

Alternatively, rate dependencies on substrate and nucleotide concentrations were fit to a Hill-type Equation 4,

$$v = v_0 + (v_L - v_0)/(1 + K_L/[L]^h), \quad \text{(Eq. 4)}$$

where L is S or N, v_L is the rate at infinite [L], and h is the Hill coefficient. The value of v_0 was set to zero when L was substrate, and the value of h was set to unity for non-cooperative binding.

Isothermal titration calorimetry (ITC) data were analyzed with a MicroCal ITC subroutine in Origin 7.0 software using a single-binding-site model. Thermodynamic parameters were calculated from the standard relationship, $\Delta G = RT\ln K_N = \Delta H - T\Delta S$.

Results

Effects of Ap_nAs *on CBS-PPases at a Fixed* Mg^{2+} *Concentration*—Figure 1 shows the concentration dependencies of the effects of four Ap_nAs with $n = 3-6$ on the activities of three CBS-PPases measured at fixed substrate ($MgPP_i$) and Mg^{2+} concentrations (50 μM and 5 mM, respectively). Nanomolar concentrations of Ap_nAs caused marked activation in all cases, except that Ap_3A was effective with *cp*PPase at micromolar concentrations.

Analyses of the dependencies shown in Figure 1 and of similar dependencies measured at different substrate concentrations (1 and 300 μM) were initially done using Equation 4. The value of the Hill coefficient was indistinguishable from unity (1 ± 0.05) at all substrate concentrations for Ap_nAs with $n = 4-6$. In contrast, Ap_3A bound cooperatively ($h = 1.4-1.7$) at all substrate concentrations. Accordingly, the data for Ap_3A were analyzed with Equations 1 and 4 in their general forms, whereas Equation 4 with $h = 1$ was used for the other Ap_nAs. The parameter values derived from this analysis are summarized in Tables 1 and 2.

The values of the activation factor (v_N/v_0) and their trends with changing polyphosphate length and substrate concentration were similar for the three enzymes. The maximal value of v_N/v_0 was greater at low than at high substrate concentrations. In the presence of 300 μM substrate, which is in excess of the respective Michaelis constants (32), v_N/v_0 approached a value of ~2 in all cases.

The apparent binding affinities of the nucleotides could be compared on the basis of the average binding constant ($\sqrt{K_{N1}K_{N2}}$) for Ap_3A and respective K_N values for the other dinucleotides. As Tables 1 and 2 make clear, the binding affinity estimated at 50 μM substrate was markedly lower for Ap_3A compared to other dinucleotides for all CBS-PPases. Increasing *n* did not affect *dh*PPase affinity, but it did slightly increase *cn*PPase affinity and decrease *cp*PPase affinity. Increasing substrate concentration had opposite effects on the affinity of Ap_3A and Ap_4A for *dh*PPase and *cp*PPase (increased) and *cn*PPase (decreased). Of note, *cp*PPase exhibited much lower affinity for all dinucleotides compared to other CBS-PPases.

Surprisingly, neither dinucleotide at a concentration up to 10 μM affected activities of *el*PPase or *mt*PPase measured with 50 μM substrate. These CBS-PPases differ from those described above by having no DRTGG domain in their regulatory regions, which are formed by only two CBS domains. Moreover, 10 μM Ap_4A did not affect the concentration dependence of ADP inhibition of *el*PPase or *mt*PPase (data not shown), indicating that the dinucleotide is unable to interact with the ADP-binding site.

Dependence of CBS-PPase Activation on Mg^{2+} *Concentration*—Given that cooperativity in CBS-PPases is Mg^{2+} dependent (32), measurements analogous to those illustrated in Figure 1 were conducted for two representative dinucleotides, Ap_3A and Ap_4A, over a 0.05−20 mM Mg^{2+} concentration range; substrate concentration was fixed at 50 μM. The results of these experiments (Fig. 2) indicated that Ap_3A bound with positive cooperativity and Ap_4A bound non-cooperatively to all CBS-PPases at all Mg^{2+} concentrations. In only one case (*dh*PPase with Ap_3A), the degree of cooperativity showed a pronounced dependence on [Mg^{2+}], as evidenced by the opposite effects of Mg^{2+} on K_{N1} and K_{N2} (Fig. 2).

In most cases (except for *dh*PPase with Ap_4A), Mg^{2+} modulated dinucleotide binding, with the direction of the effect depending on both the nature of the nucleotide and the CBS-PPase origin (Figs 2 and 3). Mg^{2+} generally stimulated Ap_3A binding, except for *dh*PPase, where it exerted the opposite effect on K_{N1} (Fig. 2). Mg^{2+} exhibited a full range of effects on Ap_4A binding (Fig. 2): stimulation (*cp*PPase), suppression (*cn*PPase), and no effect (*dh*PPase). The effect of Mg^{2+} on dinucleotide binding could be described by Equation 3, yielding the parameter values summarized in Table 3. The values of K_M governing the Mg^{2+} effects were in the millimolar range and were similar for both steps of Ap_3A binding and Ap_4A binding for a given CBS-PPase.

The degree of activation (v_N/v_0) of *dh*PPase and *cn*PPase by Ap_3A and Ap_4A demonstrated no or only small variations with Mg^{2+} concentration (Fig. 2). In contrast, activation of *cp*PPase showed a bell-shaped dependence (Ap_3A) or markedly

decreased (Ap_4A) with increasing Mg^{2+} concentration.

Analysis of CBS-PPase Activation in Terms of Michaelis-Menten Parameters—As previously reported, the rate of $MgPP_i$ hydrolysis by CBS-PPases does not obey Michaelis-Menten kinetics, requiring the use of a more complex equation with two Michaelis constants (32). Their ratio, K_{m2}/K_{m1}, was less than four, and the Hill coefficient was greater than one, indicating positive kinetic cooperativity.

Surprisingly, Ap_3A and Ap_4A completely abolished or markedly suppressed the kinetic cooperativity in *dh*PPase, *cn*PPase and *cp*PPase, as indicated by a Hill coefficient with a value close to 1 (Table 4 and Fig. 3). That the *h* value is greater than 1 for *cp*PPase in the presence of Ap_3A likely reflects incomplete saturation of this enzyme by the dinucleotide, which binds much more weakly to *cp*PPase compared with the other CBS-PPases (Table 1).

The kinetics of activation by Ap_4A was investigated over a range of Mg^{2+} concentrations (Fig. 3). The results showed that 10 μM activator increased k_{cat}, decreased the Michaelis constant, and abolished kinetic cooperativity. Again the largest effects were observed with *cp*PPase, which was therefore explored in greater detail.

The effects of three Ap_nAs on the Mg^{2+} concentration dependence of k_{cat} for *cp*PPase were qualitatively similar, with Ap_4A being a somewhat more efficient activator (Fig. 4). Mg^{2+} induced a transition from low to high activity over a narrow range of concentrations, requiring a term with $[Mg^{2+}]^2$ in the corresponding equation (see Fig. 3 legend) (32). All three activators increased the limiting value of k_{cat} at infinite $[Mg^{2+}]$ ($k_{cat,M}$) and decreased the Mg^{2+}-binding constant (K_M) approximately 2-fold (Table 5). Most surprisingly, Ap_nA binding conferred catalytic activity to the otherwise inactive *cp*PPase at low $[Mg^{2+}]$ (see $k_{cat,0}$ values in Table 5). The activity of Ap_4A-activated *cp*PPase in these conditions approached its maximum activity observed at high $[Mg^{2+}]$ in the absence of Ap_4A (Fig. 4).

Figure 5 illustrates the concentration dependence of *cp*PPase activation by Ap_4A in the presence of 0.5 mM Mg^{2+}, analyzed in terms of k_{cat} and K_m values. The value of k_{cat} increased ~7.5-fold (from 240 ± 100 to 1800 ± 100 s^{-1}), K_{m1} decreased ~18-fold (from 70 ± 10 to 4 ± 1 μM), and K_{m2} changed insignificantly with increasing Ap_4A concentration from 0 to 5 μM. The Ap_4A binding constant estimated from k_{cat} and K_{m1} dependencies was 0.04 ± 0.01 and 1.7 ± 1.0 μM, respectively. Because k_{cat} and K_m dependencies report on Ap_4A binding to substrate-free enzyme and enzyme-substrate complex, respectively, a likely implication is that Ap_4A and the first-bound substrate molecule mutually stabilize binding of each other to *cp*PPase 20−40-fold.

Thermodynamics and Stoichiometry of Nucleotide Binding to CBS-PPases—Using ITC allowed the direct measurement of changes in free energy (ΔG), enthalpy (ΔH), and entropic free energy ($T\Delta S$) components of nucleotide binding to CBS-PPases. A typical titration profile is shown in Figure 6A. The results of similar titrations performed with different CBS-PPases and nucleotides are summarized in Figure 6B and Table 6. Because of the very tight binding, K_N and, accordingly, $T\Delta S$ values could not be estimated with adequate precision in most Ap_nA titrations. The most important finding was that ΔH, as calculated per mole of nucleotide, was nearly 2-times greater for Ap_4A and Ap_5A than for Ap_3A and the mononucleotides. This effect correlated with a 2-fold lower binding stoichiometry for Ap_4A and Ap_5A compared with that for mononucleotides and Ap_3A. Where K_N (and hence ΔG) values were available, the free energy change of nucleotide binding was dominated by ΔH, with a significant contribution from $T\Delta S$, likely owing to a hydrophobic effect. The K_N values derived from ITC measurements are in a fair agreement with those obtained from nucleotide effects on activity (see Ref. 32 for mononucleotides and Table 1 for Ap_3A). It should be noted that ITC measurements can hardly distinguish positive binding cooperativity and yield an average ΔH value for all binding sites.

No ITC signal was observed when the DRTGG-domain–lacking *el*PPase or *mt*PPase was titrated with up to 10 μM Ap_4A, consistent with the inability of Ap_4A to activate these CBS-PPases. In contrast, with one exception (AMP with *el*PPase), mononucleotides produced similar ITC effects on CBS-PPases regardless of the presence or absence of a DRTGG domain (Table 6). These findings suggest that the DRTGG domain is required for binding of diadenosine polyphosphates, but not monoadenosine polyphosphates, to CBS-PPases.

Discussion

CBS domains, found in many proteins, are known for their ability to bind adenine nucleotides and in this way regulate activities of their carrier proteins. The list of regulating adenine nucleotides includes AMP, ADP, ATP, S-adenosyl methionine, NADH, and analogs of AMP and ATP (27). Examples of less common CBS domain ligands include Mg^{2+} (37), DNA, and RNA (38, 39). We earlier reported that crystals of the isolated dimeric regulatory region of *cp*PPase grown in the presence of Ap_4A contains one Ap_4A molecule per dimer bridging two pairs of CBS domains, whereas each CBS domain pair binds an AMP molecule (33). We also found that Ap_4A induces a significant opening of the interface compared with the AMP-bound form. The results reported above extend these earlier findings by showing that (a) Ap_nAs with n = 3 to 6 bind three CBS-PPases with nanomolar affinity and activate them *in vitro*; (b) Ap_nA binding is only observed in CBS-PPases that have an intercalating DRTGG domain in the regulatory region; (c) unlike common adenine nucleotides, long-chain Ap_nAs (n > 3) abolish kinetic cooperativity (non-Michaelian behavior) in CBS-PPases. The unique features of Ap_nA complexes of CBS-PPases compared with those of their complexes with mononucleotides and complexes of other CBS proteins with their regulating ligands are described below. Notably, Ap_nAs have not been reported as ligands for any other CBS protein.

Based on their binding properties, Ap_nAs can be divided into two groups. Ap_3A bound to all CBS-PPases cooperatively and with lower affinity, as characterized by either K_{N1} and K_{N2}, or their average value ($\sqrt{K_{N1}K_{N2}}$) (Table 1). The other dinucleotides (n = 4–6) bound non-cooperatively and with a higher affinity that did not depend significantly on the n value (Table 2). The affinities of Ap_nAs with n = 4–6 for CBS-PPases surpassed that of adenine mononucleotides (32) by 2−3 orders of magnitude. Such high affinities are unprecedented among other CBS proteins, which generally bind their nucleotide ligands in the millimolar range. The difference in the binding affinities of the two Ap_nA groups was most pronounced with *cp*PPase, amounting to three orders of magnitude. As previously demonstrated (33), Ap_4A interacts through both of its adenine moieties with two CBS domain pairs of different subunits in *cp*PPase. Such an arrangement is also likely with Ap_5A and Ap_6A, consistent with their similar ΔH values and binding stoichiometries, determined from ITC measurements (Table 6). In contrast, ΔH for Ap_3A was half that of Ap_5A and Ap_6A and the binding stoichiometry was 2-fold higher, similar to values for mononucleotides (Table 6). These observations likely indicate that Ap_3A predominantly binds CBS-PPases through only one adenine moiety.

The binding affinities of Ap_nAs showed a complex dependence on substrate and metal cofactor concentrations. At a constant Mg^{2+} concentration, substrate increased the binding affinities of *dh*PPase and *cp*PPase for all Ap_nAs, but exerted an opposite effect on *cn*PPase (Tables 1 and 2). Accordingly, Ap_3A (Table 4) and Ap_4A (Fig. 3) decreased the average Michaelis constant ($\sqrt{K_{m1}K_{m2}}$ and K_m). The effect of Ap_3A on $\sqrt{K_{m1}K_{m2}}$ for *cp*PPase measured in the presence of 5 mM Mg^{2+} was quite modest, but keeping in mind the bell-shaped dependence of $\sqrt{K_{m1}K_{m2}}$ on [Mg^{2+}] for this enzyme in the absence of adenine nucleotides (Fig. 3), one would expect, by analogy, greater effects of Ap_3A at low [Mg^{2+}].

However, the most striking effect of Ap_nAs on substrate binding was abolition of kinetic cooperativity. This effect was observed with both Ap_3A and Ap_4A, representing the two dinucleotide groups, and might be explained by two different mechanisms. First, the effectors may disrupt the communication between active sites, allowing them to function independently. Alternatively, the dinucleotides may induce asymmetry in the enzyme dimer such that only one active site operates in the dimer (ultimate negative cooperativity). Determining the three-dimensional structure of the enzyme with bound dinucleotide would make it possible to discriminate between these alternative explanations.

Mg^{2+} effects on nucleotide binding also varied depending on the enzyme (Fig. 2) and differed from those observed with adenine mononucleotides (32). With Ap_3A, values of K_{N1} and K_{N2} for *dh*PPase changed in different directions, decreasing the degree of cooperativity at low [Mg^{2+}] (Fig. 2A). No bound Mg^{2+} ion was observed in the structure of the regulatory region of *cp*PPase (33), suggesting that the modulatory Mg^{2+} resides in the active site. Notable in this regard, three Mg^{2+} ions per active site participate in catalysis among homologous non-regulated Family II PPases (24, 40). The effects of Mg^{2+} on

nucleotide binding may, in part, be a consequence of its effects on substrate binding, as these measurements were carried out at a non-saturating substrate concentration (50 μM).

All Ap_nAs activated CBS-PPases under the conditions tested owing to favorable changes in both k_{cat} and the average Michaelis constant ($\sqrt{K_{m1}K_{m2}}$) (Table 4 and Fig. 3). Accordingly, the degree of activation was greater at low substrate concentrations (Table 1) and varied from several-fold to several tens of fold. The largest effects were observed with *cp*PPase. Based on its k_{cat} and K_m values (Fig. 3), this enzyme is predicted to be activated by Ap_4A in the presence of 1 mM Mg^{2+} by a factor of ~51 and ~19 at substrate concentrations of 1 and 10 μM, respectively. At low [Mg^{2+}], the activating effect of Ap_nA is dominated by k_{cat}, especially with *cp*PPase (Fig. 4, Table 5). In this enzyme, k_{cat} is strongly Mg^{2+}-dependent and Ap_nA markedly released this dependence by allowing catalysis in the enzyme with a vacant Mg^{2+} site and by somewhat increasing its affinity for Mg^{2+} (Table 5). In this respect, Ap_nAs partially substitute for Mg^{2+} as an enzyme activator.

Qualitatively similar activating effects on CBS-PPases were previously observed with ATP (31, 32), though ATP effects were smaller in size and required much higher effector concentrations. A further difference is that ATP bound cooperatively, like Ap_3A. The effects of ATP and Ap_3A are thus similar in many aspects. As noted above, activator binding induces significant opening of the CBS domain interface (33). Such opening can be achieved upon binding of a single molecule of Ap_4A or a longer dinucleotide that binds to both subunits of CBS-PPase through two adenine moieties. Structure modeling of the *cp*PPase regulatory region indicated that the polyphosphate chain of Ap_3A is too short for this binding mode. In this case, and with ATP, interface opening apparently results from repulsion between two molecules of the effector bound to different subunits.

The requirement for an intercalating DRTGG domain for Ap_nA binding to CBS domains provides another interpretive challenge. In the structure of the regulatory region and the modeled structure of the whole *cp*PPase, both the DRTGG domain and CBS domain pairs participate in forming the subunit interface (33). DRTGG-domain–containing CBS-PPases apparently have a larger binding cavity for the regulating ligands or increased flexibility of the CBS domains at the expense of their smaller contribution to the subunit contact area, allowing them to accommodate more bulky Ap_nA molecules. This interpretation is supported by data showing that the DRTGG-domain–deficient *el*PPase (32) and *mt*PPase (31) bind ATP with an affinity 1−2 orders of magnitude lower than that of the less bulky AMP and ADP. In contrast, no such discrimination is observed in DRTGG-domain–containing CBS-PPases (32). Notably, the primary structures of the CBS domains in DRTGG-domain–deficient CBS-PPases (Fig. 7) do not contain specific mutations that would disallow their binding of Ap_nAs. Despite a generally low degree of residue conservation in CBS domains, all residues involved in nucleotide binding are found in at least one of the DRTGG-domain–deficient CBS-PPases. Based on these considerations, Ap_nAs are not expected to bind with comparable affinity to the numerous other CBS proteins that lack a DRTGG or other intercalating domain.

Ap_nA binding is expected to significantly change CBS-PPase activity *in vivo*, particularly under low-energy conditions, when the concentration of the alternative activator, ATP, is low. Although basal intracellular levels of Ap_nAs are four orders of magnitude lower than those of adenine mononucleotides, Ap_nA concentrations can rise by two orders of magnitude under stress conditions (41, 42). Also taking into consideration their extraordinarily high affinity, Ap_nAs could be expected to efficiently compete with mononucleotides for CBS-PPase binding in these circumstances. An increase in CBS-PPase activity is expected to decrease the concentration of PP_i and thus release PP_i-mediated inhibition of numerous biosynthetic reactions in which PP_i is produced as a byproduct (43). That the affinity of CBS-PPases for Ap_nAs markedly surpasses that of all known Ap_nA-binding proteins suggests that this enzyme is a dominant target through which Ap_nAs fulfill their stress-response–related functions in bacteria.

Acknowledgment

The authors thank Dr. P. Semenyuk for help with ITC measurements.

Conflict of Interest

The authors declare no conflict of interest.

Author Contributions—VAA designed, performed and analyzed the experiments, and contributed to writing the manuscript. AS designed and constructed vectors, expressed and purified proteins, and performed bioinformatics analyses. HKT performed ITC experiments with *dh*PPase. VKO supervised ITC experiments and data analysis. RL designed and supervised the experiments. AAB designed and analyzed experiments and wrote the manuscript. All authors reviewed the results and approved the final version of the manuscript.

REFERENCES

1. Reiss, J. R., and Moffat, J. G. (1965) Dismutation reactions of nucleoside polyphosphates. III. The synthesis of α,ω-dinucleoside 5′-polyphosphates. *ACS Journal*, **30**, 3381−3387

2. Fraga, H., and Fontes, R. (2011) Enzymatic synthesis of mono and dinucleoside polyphosphates. *Biochim. Biophys. Acta* **1810**, 1195−1204

3. Zamecnik, P. C., Stephenson, M. L., Janeway, C. M., and Randerath, K. (1966) Enzymatic synthesis of diadenosine tetraphosphate and diadenosine triphosphate with a purified lysyl-sRNA synthetase. *Biochem. Biophys. Res. Commun.* **24**, 91−97

4. Goerlich, O., Foeckler, R., and Holler, E. (1982) Mechanism of synthesis of adenosine(5′)tetraphospho(5′)adenosine (AppppA) by aminoacyl-tRNA synthetases. *Eur. J. Biochem*. **126,** 135–142

5. Wright, M., Boonyalai, N., Tanner, J. A., Hindley, A. D., and Miller, A. D. (2006) The duality of LysU, a catalyst for both Ap_4A and Ap_3A formation. *FEBS J.* **273,** 3534 –3544

6. Guranowski, A. (2000) Specific and nonspecific enzymes involved in the catabolism of mononucleoside and dinucleoside polyphosphates. *Pharmacol. Ther*. **87**, 117–139

7. Jiang, Y-L., Zhang, J-W., Yu, W-L., Cheng, W., Zhang, C-C., Frolet, C., Di Guilmi, A-M., Vernet, T., Zhou, C-Z., and Chen, Y. (2011) Structural and enzymatic characterization of the streptococcal ATP/diadenosine polyphosphate and phosphodiester hydrolase Spr1479/SapH. *J. Biol. Chem*. **286**, 35906–35914

8. Lee, P. C., Bochner, B. R., and Ames, B. N. (1983) AppppA, heat shock stress, and cell oxidation. *Proc. Acad. Sci USA* **80**, 7496–7500

9. Bochner, B. R., Zylicz, M., and Georgopoulos, C. (1986) *Escherichia coli* DnaK protein possesses a 5′-nucleotidase activity that is inhibited by AppppA. *J. Bacteriol*. **168**, 931–935

10. Varshavsky, A. (1988) Diadenosine 5′,5′′′-P^1,P^4-tetraphosphate: a pleiotypically acting alarmone. *Cell* **34**, 711–712

11. Tanner, J. A., Wright, M., Christie, E. M., Preuss, M. K., and Miller, A. D. (2006) Investigation into the interactions between diadenosine 5',5'''-P1,P4-tetraphosphate and two proteins: molecular chaperone GroEL and cAMP receptor protein. *Biochemistry* **45,** 3095–3106

12. Tshori, S., Razin, E., and Nechushtan, H. (2013) Amino-acyl tRNA synthetases generate dinucleotide polyphosphates as second messengers: functional implications. *Top. Curr. Chem*, **344**, 10–12

13. Sillero, M. A. G., de Diego, A., Osorio, H., and Sillero, A. (2002) Dinucleoside polyphosphates stimulate the primer independent synthesis of poly(A) catalyzed by yeast poly(A) polymerase. *Eur. J. Biochem*. **269**, 5323–5329

14. Nishimura, A., Moriya,S., Ukai, H., Nagai, K., Wacho, M., and Yamada, Y. (1997) Diadenosine 5',5'''-P1,P4-tetraphosphate (Ap_4A) controls the timing of cell division in *Escherichia coli*. *Genes Cells* **2**, 401–413

15. Gómez-Villafuertes, R., Pintor, J., Gualix, J., and Miras-Portugal, M. T. (2004) GABA modulates presynaptic signalling mediated by dinucleotides on rat synaptic terminals. *J. Pharmacol. Exp. Ther*. **308**, 1148–1157

16. Vartanian, A. A., Suzuki, H., and Poletaev, A. I. (2003) The involvement of diadenosine 5',5'''-P1,P4-tetraphosphate in cell cycle arrest and regulation of apoptosis. *Biochem Pharmacol*. **65**, 227–235

17. Giraldez, L., Díaz-Hernández, M., Gómez-Villafuertes, R., Pintor, J., Castro, E., and Miras-Portugal, M. T. (2001) Adenosine triphosphate and diadenosine pentaphosphate induce $[Ca^{2+}]_i$ increase in rat basal ganglia aminergic terminals. *J. Neurosci. Res.* **64**, 174–182
18. Conant, A.R., Theologou, T., Dihmis, W. C., and Simpson, A. W. M. (2008) Diadenosine polyphosphates are selective vasoconstrictors in human coronary artery bypass grafts cells. *Vascular Pharmacol.*, **48**, 157–164
19. Johnstone, D. B., and Farr, S. B. (1991) AppppA binds to several proteins in *Escherichia coli*, including the heat shock and oxidative stress proteins DnaK, GroEL, E89, C45 and C40. *EMBO J.* **10**, 3897–3904
20. Guo, W., Azhar, M. A., Xu, Y., Wright, M., Kamal, A, and Miller, A. D. (2011) Isolation and identification of diadenosine 5′,5‴-P^1,P^4-tetraphosphate binding proteins using magnetic bio-panning. *Bioorg. Med. Chem. Lett.* **21**, 7175–7179
21. Azhar, M. A., Wright, M., Kamal, A., Nagy, J., and Miller, A. D. (2014) Biotin-c10-AppCH2ppA is an effective new chemical proteomics probe for diadenosine polyphosphate binding proteins. *Bioorg. Med. Chem. Lett.* **24**, 2928–2933
22. Marques, A. F., Teixeira, N. A., Gambaretto, C., Sillero, A., and Sillero M. A. **(**1998) IMP-GMP 5′-nucleotidase from rat brain: activation by polyphosphates. *J. Neurochem.* **71**, 1241–1250
23. Kajander, T. K., Kellosalo, J., and Goldman, A. (2013) Inorganic pyrophosphatases: one substrate, three mechanisms. *FEBS Lett*. **587**, 1863–1869
24. Parfenyev, A. N., Salminen, A., Halonen, P., Hachimori, A., Baykov, A. A., and Lahti, R. (2001) Quaternary structure and metal-ion requirement of family II pyrophosphatases from *Bacillus subtilis, Streptococcus gordonii* and *Streptococcus mutans*. *J. Biol. Chem*. **276***,* 24511–24518
25. Bateman, A. (1997) The structure of a domain common to archaebacteria and the homocystinuria disease protein. *Trends Biochem. Sci.* **22**, 12–13
27. Baykov A. A., Tuominen H. K., and Lahti R. (2011) The CBS domain: a protein module with an emerging prominent role in regulation. *ACS Chem. Biol*. **6**, 1156**–**1163
26. Ereño-Orbea, J., Oyenarte, I. and Martìnez-Cruz, L. A. (2013) CBS domains: ligand binding sites and conformational variability. *Arch. Biochem. Biophys.* **540**, 70–81
28. Kemp, B. E. (2004) Bateman domains and adenosine derivatives form a binding contract. *J. Clin. Invest.* **113**, 182–184
29. Ignoul, S., and Eggermont, J. (2005) CBS domains: structure, function, and pathology in human proteins. *Am. J. Physiol. Cell Physiol*. **289**, C1369–1378
30. Scott, J. W., Hawley, S. A., Green, K. A., Anis, M., Stewart, G., Scullion, G. A., Norman, D. G., and Hardie, D. G. (2004) CBS domains form energy-sensing modules whose binding of adenosine ligands is disrupted by disease mutations. *J. Clin. Invest*. **113**, 274–284
31. Jämsen, J., Tuominen, H., Salminen, A., Belogurov, G. A., Magretova, N. N., Baykov, A. A., and Lahti, R. (2007) A CBS domain-containing pyrophosphatase of *Moorella thermoacetica* is regulated by adenine nucleotides. *Biochem. J*. **408**, 327–353
32. Salminen A., Anashkin V. A., Lahti M., Tuominen H. K., Lahti R., Baykov A. A. (2014) Cystathionine ß-synthase (CBS) domains confer multiple forms of Mg^{2+}-dependent cooperativity to Family II pyrophosphatases. *J. Biol. Chem.* **289**, 22865–22876
33. Tuominen, H., Salminen, A., Oksanen, E., Jämsen, J., Heikkilä, O., Lehtiö, L., Magretova, N. N., Goldman, A., Baykov, A. A., and Lahti, R. (2010) Crystal structures of the CBS and DRTGG domains of the regulatory region of *Clostridium perfringens* pyrophosphatase complexed with the inhibitor, AMP, and activator, diadenosine tetraphosphate. *J. Mol. Biol*. **398**, 400–413
34. Jämsen, J., Baykov, A. A., and Lahti, R. (2012) Fast kinetics of nucleotide binding to *Clostridium perfringens* family II pyrophosphatase containing CBS and DRTGG domains *Biochemistry (Moscow)* 77, 165–170
35. Baykov, A. A., and Avaeva, S. M. (1981) A simple and sensitive apparatus for continuous monitoring of orthophosphate in the presence of acid-labile compounds. *Anal. Biochem*. **116**, 1–4
36. Baykov, A. A., Bakuleva, N. P., and Rea, P. A. (1993) Steady-state kinetics of substrate hydrolysis by vacuolar H^+-pyrophosphatase. A simple three-state model. *Eur. J. Biochem*. **217**, 755–762

37. Hattori, M., Tanaka, Y., Fukai, S., Ishitani, R., and Nureki, O. (2007) Crystal structure of the MgtE Mg^{2+} transporter. *Nature* **448**, 1072–1075
38. McLean, J. E., Hamaguchi, N., Belenky, P., Mortimer, S. E., Stanton, M., and Hedstrom, L. (2004) Inosine 5′-monophosphate dehydrogenase binds nucleic acids in vitro and in vivo. *Biochem. J.* **379**, 243–251
39. Aguado-Llera, D., Oyenarte, I., Martínez-Cruz, L. A., and Neira, J. L. (2010) The CBS domain protein MJ0729 of *M. jannaschii* binds DNA. *FEBS Lett*. **584**, 4485–4489
40. Fabrichniy, I. P., Lehtiö, L., Tammenkoski, M., Zyryanov, A. B., Oksanen, E. J., Baykov, A. A., Lahti, R., and Goldman, A. (2007) A trimetal site and ground-state substrate distortion mark the active site of family II inorganic pyrophosphatase. *J. Biol. Chem.* **282**, 1422–1431
41. Garrison, P.N., and Barnes, L.D. (1992) Determination of dinucleoside polyphosphates, in *Ap4A and Other Dinucleoside Polyphosphates* (McLennan, A.G., ed.), CRC Press, Boca Raton, pp. 29–61
42. Plateau, P., and Blanquet, S. (1994) Dinucleoside oligophosphates in micro-organisms. *Adv. Microb. Physiol*. **36**, 81–109
43. Heinonen, J. K. (2001) *Biological Role of Inorganic Pyrophosphate*, pp. 123−188, Kluwer Academic Publishers, London

FOOTNOTES

*This work was supported by Academy of Finland Grant 139031 and Russian Foundation for Basic Research Grants 12-04-01002 and 15-04-0482815.

[1] To whom correspondence may be addressed: Dept. of Biochemistry, University of Turku, Vatselankatu 2, FIN-20014 Turku, Finland. Tel.: 358-2353-6845; Fax: 358-2353-6860; E-mail: reijo.lahti@utu.fi.

[2] To whom correspondence may be addressed: Dept. of Protein Chemistry, Belozersky Institute of Physico-Chemical Biology, Lomonosov Moscow State University, Moscow 119992, Russia. Tel.: 7-495-939-5541; Fax: 7-495-939-0358; E-mail: baykov@genebee.msu.su.

[3] The abbreviations used are: Ap_nA, 5',5-P^1,P^n-diadenosine polyphosphate with *n* phosphate residues; CBS, cystathionine β-synthase; CBS-PPase, CBS domain-containing pyrophosphatase; *cn*PPase, *C. novyi* pyrophosphatase; *cp*PPase, *C. perfringens* pyrophosphatase; *dh*PPase, *D. hafniense* pyrophosphatase; *el*PPase, *E. lenta* pyrophosphatase; *mt*PPase, *M. thermoacetica* pyrophosphatase; PPase, pyrophosphatase; Tes, 2-{[2-hydroxy-1,1-bis(hydroxymethyl)ethyl]amino}ethanesulfonic acid.

FIGURE LEGENDS

FIGURE 1. **Concentration dependencies of the effects of Ap_nAs on the activity of three CBS-PPases measured at fixed concentrations of substrate (50 μM $MgPP_i$) and Mg^{2+} (5 mM).** The lines show the best fits of Equations 1 or 4 (see text for details). Activity without nucleotides (220, 350 and 800 s^{-1} for *dh*PPase, *cn*PPase and *cp*PPase, respectively) was taken as unity. *dh*, *dh*PPase; *cn*, *cn*PPase; *cp*, *cp*PPase.

FIGURE 2. **Mg^{2+} concentration dependence of CBS-PPase activation by Ap_3A (*left*) and Ap_4A (*right*).** The panels show (from top to bottom)the activation factor K_{N1} (○) and K_{N2} (●) values and Hill coefficients. The K_{N1} and K_{N2} lines show the best fits to Equation 3. The horizontal dotted lines (h = 1) mark the boundary between positive and negative cooperativity. *dh*, *dh*PPase; *cn*, *cn*PPase; *cp*, *cp*PPase.

FIGURE 3. **Lack of kinetic cooperativity in CBS-PPases in the presence of 10 μM Ap_4A.** The panels show (from top to bottom) the catalytic constant k_{cat}, the Michaelis constant K_m, and the Hill coefficient h. The dashed lines and corresponding points refer to the early-estimated parameter values in the absence of Ap_4A (32); K_m values refer to the average Michaelis constants ($\sqrt{K_{m1}K_{m2}}$) in this case. The horizontal dotted lines (h = 1) mark the boundary between positive and negative cooperativity. K_m values are measured in terms of the $MgPP_i$ complex. *dh*, *dh*PPase; *cn*, *cn*PPase; *cp*, *cp*PPase.

FIGURE 4. **Mg^{2+} concentration dependence of k_{cat} for *cp*PPase measured in the presence of 50 μM Ap_3A or 10 μM Ap_4A or Ap_5A.** Values of k_{cat} were fit to the equation $k_{cat} = k_{cat,0} + (k_{cat,M} - k_{cat,0})/\{1 + (K_M/[M])^2\}$, where $k_{cat,0}$ and $k_{cat,M}$ are the limiting values of k_{cat} at zero and infinite Mg^{2+} concentrations, respectively, and K_M is the metal-binding constant.

FIGURE 5. **Ap_4A concentration dependence of kinetic cooperativity in *cp*PPase in the presence of 0.5 mM Mg^{2+}.** Notations are as in Figure 4. Values of k_{cat} were fit to the equation $k_{cat} = k_{cat,0} + (k_{cat,N} - k_{cat0})/(1 + K_N/[M])$, where $k_{cat,0}$ and $k_{cat,M}$ are the limiting values of k_{cat} at zero and infinite Ap_4A concentrations, respectively, and K_N is the nucleotide-binding constant. The line for K_{m1} shows the best fit to Equation 3.

FIGURE 6. **ITC measurements of nucleotide binding to CBS-PPases.** *A*, Typical raw data for successive injections of Ap_4A into *dh*PPase solution. *B*, Integrated heats for titration of four CBS-PPases by mono- and dinucleotides after correction for dilution. Enzyme dimer concentration was 4 μM (*dh*PPase), 5 μM (*cn*PPase), 3.5 μM (*cp*PPase), or 2.5 μM (*el*PPase). The lines show the best fits for a single-binding–site model.

FIGURE 7. **Aligned amino acid sequences of the two CBS domains of the characterized CBS-PPases.** Amino acid residues making contacts with Ap_4A or AMP in the crystal structures of *cp*PPase (33) are shown in boxes. Consensus residues based on 180 CBS-PPase sequences are indicated in the two bottom lines. Residue numbering is for full-length *cp*PPase. Consensus residues for different levels of identity are indicated below the set of sequences.

TABLE 1
Kinetic parameters for activation of three CBS-PPases by Ap_3A in the presence of 5 mM Mg^{2+}

Enzyme	[$MgPP_i$]	v_N/v_0[a]	K_{N1}	K_{N2}	$\sqrt{K_{N1}K_{N2}}$	$4K_{N1}/K_{N2}$	h
	μM			*nM*			
*dh*PPase	1	32 ± 6	460 ± 80	100 ± 20	213 ± 5	18 ± 7	1.60 ± 0.05
	50	2.54 ± 0.01	82 ± 6	30 ± 2	50.0 ± 0.4	10.8 ± 1.4	1.51 ± 0.02
	300	1.78 ± 0.03	12 ± 4	4 ± 1	7.1 ± 0.4	12 ± 8	1.50 ± 0.10
*cn*PPase	1	5.1 ± 0.1	19 ± 1	12 ± 1	14.8 ± 0.3	7 ± 1	1.42 ± 0.04
	50	2.67 ± 0.05	41 ± 8	22 ± 4	30 ± 1	7 ± 3	1.43 ± 0.07
	300	1.77 ± 0.01	55 ± 9	22 ± 4	35.2 ± 0.9	6.3 ± 1.6	1.40 ± 0.04
*cp*PPase	1	6.8 ± 0.1	26000 ± 4000	3400 ± 600	9000 ± 300	31 ± 10	1.66 ± 0.06
	50	2.25 ± 0.05	12000 ± 5000	1500 ± 700	4200 ± 200	31 ± 29	1.69 ± 0.12
	300	2.24 ± 0.02	1800 ± 0.2	700 ± 100	1130 ± 30	10 ± 3	1.50 ± 0.05

[a] v_N and v_0 are activities extrapolated to infinite concentration of the variable nucleotide and measured in the absence of any nucleotide, respectively.

TABLE 2
Kinetic parameters for activation of three CBS-PPases by diadenosine polyphosphates with *n* = 4−6 in the presence of 5 mM Mg^{2+}[a]

Enzyme/Dinucleotide	[$MgPP_i$]	v_N/v_0[b]	K_N[c]
	μM		*nM*
***dh*PPase**			
Ap_4A	1	18 ± 1	12.1 ± 0.3
	50	3.0 ± 0.1	4.9 ± 0.2
	300	1.91 ± 0.02	4.3 ± 0.2
Ap_5A	50	3.32 ± 0.06	5.5 ± 0.2
Ap_6A	50	2.58 ± 0.06	4.4 ± 0.3
***cn*PPase**			
Ap_4A	1	6.0 ± 0.3	3.9 ± 0.1
	50	3.14 ± 0.05	7.0 ± 0.2
	300	1.51 ± 0.01	16.5 ± 0.7
Ap_5A	50	3.03 ± 0.08	4.9 ± 0.3
Ap_6A	50	2.08 ± 0.03	3.3 ± 0.2
***cp*PPase**			
Ap_4A	1	14.7 ± 0.4	293 ± 5
	50	2.52 ± 0.03	62 ± 2
	300	2.04 ± 0.02	33 ± 1
Ap_5A	50	2.30 ± 0.03	58 ± 2
Ap_6A	50	2.04 ± 0.02	187 ± 9

[a] The value of the Hill coefficient was indistinguishable from unity in all cases.
[b] v_N and v_0 are activities extrapolated to infinite concentration of the variable nucleotide and measured in the absence of any nucleotide, respectively.
[c] This parameter is equivalent to $\sqrt{K_{N1}K_{N2}}$ in Table 1.

TABLE 3
Kinetic parameters for nucleotide activation derived from the Mg^{2+} dependencies of K_{N1} and K_{N2} for Ap_3A or K_N for Ap_4A (Fig. 2)

Enzyme	Parameter value								
	Ap_3A						Ap_4A		
	K_{N1} dependence			K_{N2} dependence					
	$K_{N1,0}$	$K_{N1,M}$	K_M	$K_{N2,0}$	$K_{N2,M}$	K_M	$K_{N,0}$	$K_{N,M}$	K_M
	nM	*nM*	*mM*	*nM*	*nM*	*mM*	*nM*	*nM*	*mM*
*dh*PPase	35 ± 2	96 ± 3	0.7 ± 0.3	75 ± 2	24 ± 1	1.5 ± 0.4	5.5 ± 0.5	5.5 ± 0.5	NA[a]
*cn*PPase	390 ± 10	41 ± 6	3.2 ± 0.7	110 ± 10	14 ± 4	5 ± 3	4.3 ± 0.3	8.6 ± 0.5	0.8 ± 0.3
*cp*PPase	59000 ± 5000	4200 ± 700	1.4 ± 0.4	5600 ± 200	640 ± 50	1.1 ± 0.2	1200 ± 200	55 ± 3	1.4 ± 0.2

[a] NA, not attendant.

TABLE 4
Kinetic parameters for PP_i hydrolysis in the presence of 50 μM Ap_3A and 5 mM Mg^{2+} estimated with Equation 2[a]

Enzyme	k_{cat}	K_{m1}	K_{m2}	$\sqrt{K_{m1}K_{m2}}$	$4K_{m1}/K_{m2}$	h
	s^{-1}	μM				
*dh*PPase	565 ± 4 (350)	1.47 ± 0.03 (26)	5.8 ± 0.3 (10)	2.9 ± 0.1 (20)	1.01 ± 0.07	1.00 ± 0.02 (1.29)
*cn*PPase	1120 ± 20 (540)	5.0 ± 0.4 (23)	18 ± 3 (80)	9.5 ± 0.6 (44)	1.1 ± 0.2	1.02 ± 0.04 (1.02)
*cp*PPase	3090 ± 20 (1080)	13 ± 1 (80)	16 ± 1 (4)	14.5 ± 0.4 (18)	3.2 ± 0.3	1.23 ± 0.02 (1.8)

[a] Values in parentheses refer to parameter values previously measured in the absence of Ap_3A (32).

TABLE 5
Kinetic parameters describing effects of Mg^{2+} on k_{cat} for *cp*PPase in the presence of diadenosine polyphosphates

Ap_nA	$k_{cat,0}$	$k_{cat,M}$	K_M
	s^{-1}	s^{-1}	*mM*
None	6 ± 13	1330 ± 20	1.07 ± 0.03
Ap_3A (50 μM)	350 ± 50	3020 ± 40	0.50 ± 0.03
Ap_4A (10 μM)	990 ± 30	3130 ± 20	0.44 ± 0.02
Ap_5A (10 μM)	500 ± 40	2800 ± 30	0.57 ± 0.03

TABLE 6
Thermodynamic parameters for nucleotide complexes of CBS-PPases obtained by isothermal calorimetry

Enzyme/ Nucleotide	K_N	*n*	ΔH	$-T\Delta S$
	μM		*kcal/mol*	*kcal/mol*
***dh*PPase**				
AMP	0.76 ± 0.25	0.79 ± 0.05	-5.6 ± 0.5	-2.7 ± 0.6
ADP	1.0 ± 0.17	0.85 ± 0.04	-5.9 ± 0.4	-2.4 ± 0.5
ATP	1.25 ± 0.11	0.80 ± 0.02	-5.8 ± 0.2	-2.4 ± 0.2
Ap_3A	0.12 ± 0.05	0.97 ± 0.02	-5.3 ± 0.2	-4.0 ± 0.3
Ap_4A		0.41 ± 0.01	-10.4 ± 0.3	
Ap_5A		0.41 ± 0.01	-10.3 ± 0.3	
***cn*PPase**				
AMP	0.91 ± 0.35	0.80 ± 0.08	-5.9 ± 0.9	-2.4 ± 1.0
Ap_3A		0.94 ± 0.01	-6.1 ± 0.1	
Ap_4A		0.44 ± 0.01	-9.7 ± 0.3	
***cp*PPase**				
AMP	0.97 ± 0.03	0.87 ± 0.06	-6.0 ± 0.6	-2.3 ± 0.7
Ap_4A		0.42 ± 0.01	-10.4 ± 0.3	
***el*PPase**				
AMP			≤0.1	
ADP	4.0 ± 0.1	0.95 ± 0.1	-4.5 ± 1.6	-2.4 ± 2.0
Ap_4A			≤0.1	

Figure 1

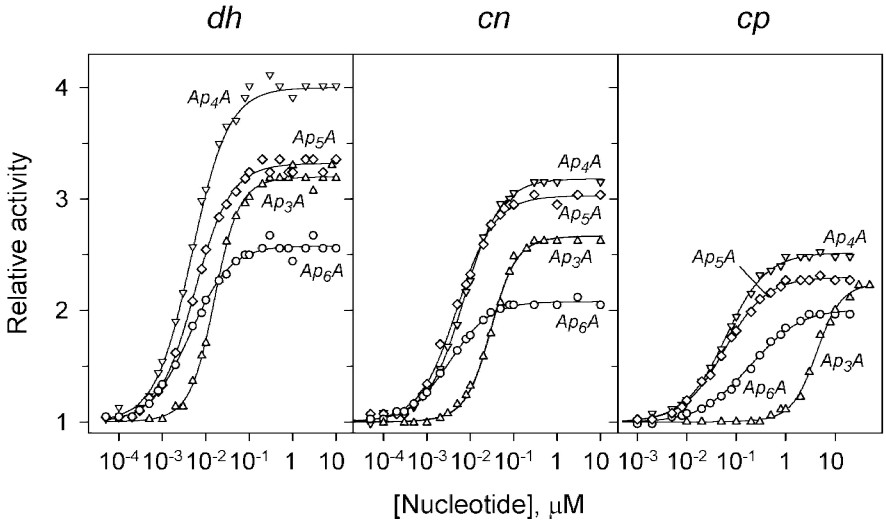
dh
cn
cp
Relative activity
[Nucleotide], μM
Ap4A
Ap5A
Ap3A
Ap6A

Figure 2

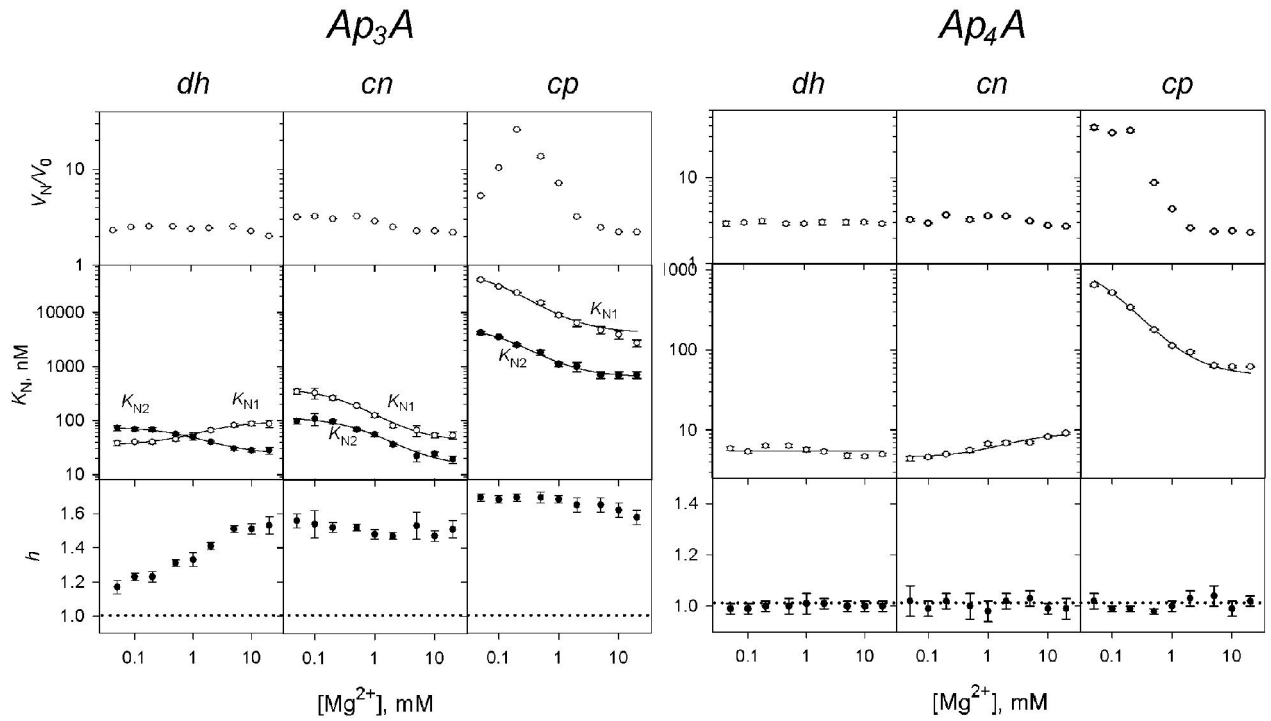

Figure 3

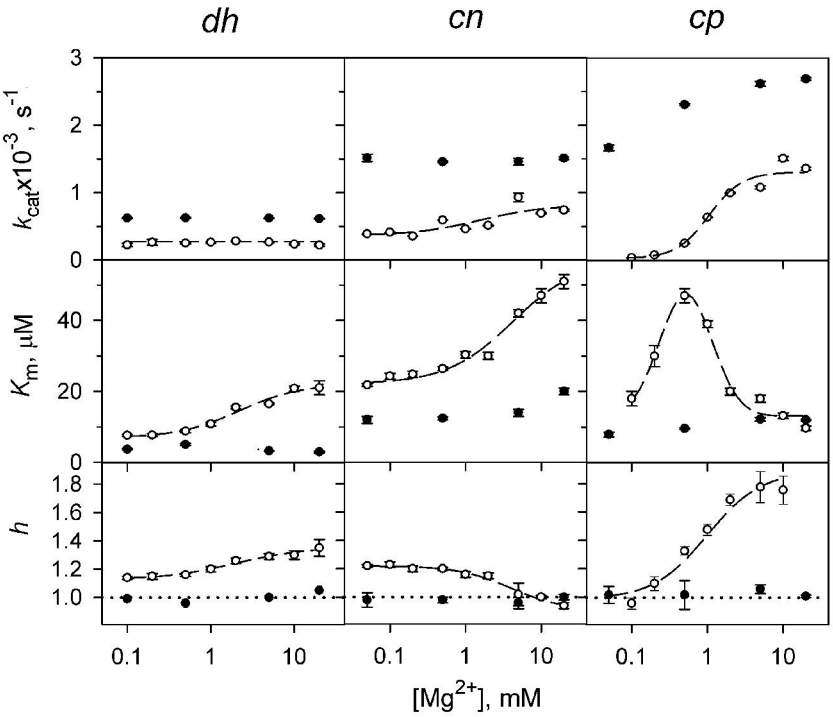

Figure 4

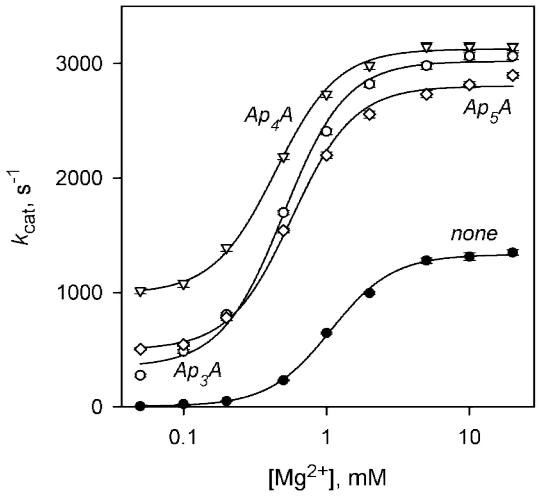

Figure 5

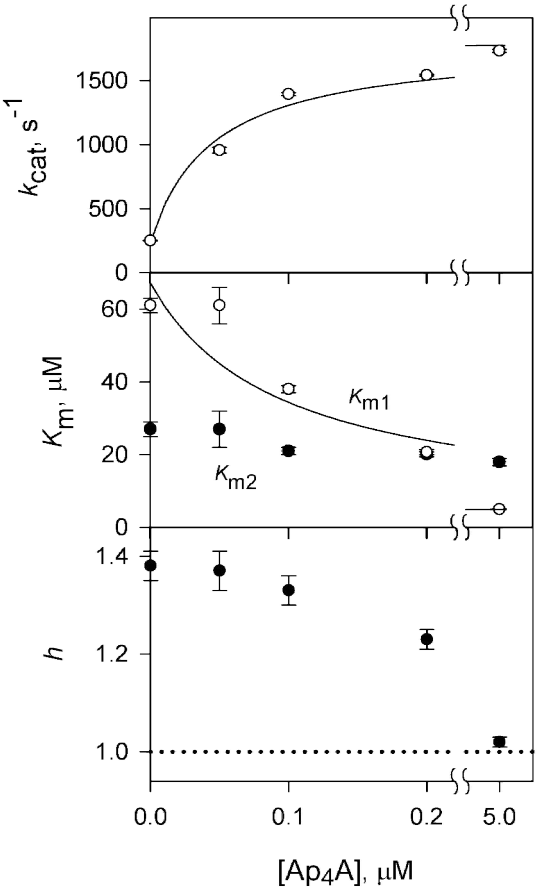
k_{cat}, s^{-1}
1500
1000
500
0
60
40
20
0
K_m, μM
K_{m1}
K_{m2}
1.4
1.2
1.0
h
0.0
0.1
0.2
5.0
[Ap4A], μM

Figure 6

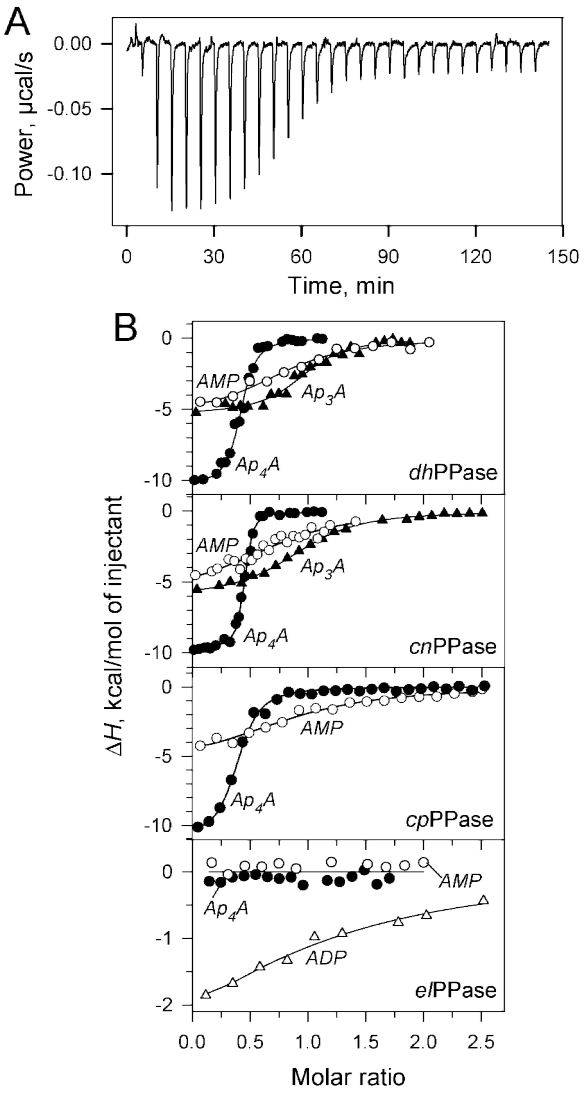
A
Power, µcal/s
0.00
-0.05
-0.10
0
30
60
90
120
150
Time, min
B
ΔH, kcal/mol of injectant
AMP
Ap3A
Ap4A
dhPPase
cnPPase
cpPPase
elPPase
ADP
0
-5
-10
-1
-2
0.0
0.5
1.0
1.5
2.0
2.5
Molar ratio

Figure 7

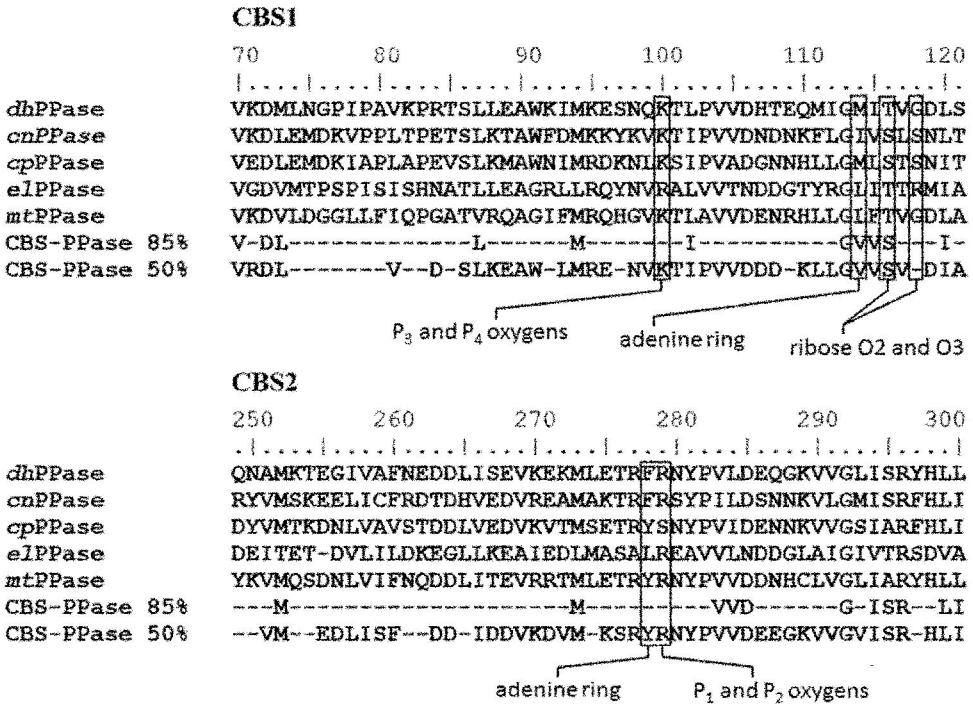
CBS1
70 80 90 100 110 120
dhPPase VKDMLNGPIPAVKPRTSLLEAWKIMKESNQKTLPVVDHTEQMIGMITVGDLS
cnPPase VKDLEMDKVPPLTPETSLKTAWFDMKKYKVKTIPVVDNDNKFLGIVSLSNLT
cpPPase VEDLEMDKIAPLAPEVSLKMAWNIMRDKNLKSIPVADGNNHLLGMLSTSNIT
elPPase VGDVMTPSPISISHNATLLEAGRLLRQYNVRALVVTNDDGTYRGLITTRMIA
mtPPase VKDVLDGGLLFIQPGATVRQAGIFMRQHGVKTLAVVDENRHLLGLFTVGDLA
CBS-PPase 85% V-DL----------L-------M---------I----------GVVS----I-
CBS-PPase 50% VRDL--------V--D-SLKEAW-LMRE-NVKTIPVVDDD-KLLGVVSV-DIA
P3 and P4 oxygens
adenine ring
ribose O2 and O3
CBS2
250 260 270 280 290 300
dhPPase QNAMKTEGIVAFNEDDLISEVKEKMLETRFRNYPVLDEQGKVVGLISRYHLL
cnPPase RYVMSKEELICFRDTDHVEDVREAMAKTRFRSYPILDSNNKVLGMISRFHLI
cpPPase DYVMTKDNLVAVSTDDLVEDVKVTMSETRYSNYPVIDENNKVVGSIARFHLI
elPPase DEITET-DVLILDKEGLLKEAIEDLMASALREAVVLNDDGLAIGIVTRSDVA
mtPPase YKVMQSDNLVIFNQDDLITEVRRTMLETRYRNYPVVDDNHCLVGLIARYHLL
CBS-PPase 85% ---M----------M----------VVD------G-ISR--LI
CBS-PPase 50% --VM--EDLISF--DD-IDDVKDVM-KSRYRNYPVVDEEGKVVGVISR-HLI
adenine ring
P1 and P2 oxygens